REPORT

Bent Bone Dysplasia-FGFR2 type, a Distinct Skeletal Disorder, Has Deficient Canonical FGF Signaling

Amy E. Merrill,[1,6,7,8] Anna Sarukhanov,[1] Pavel Krejci,[6,9,10] Brian Idoni,[7] Natalia Camacho,[1] Kristine D. Estrada,[3] Karen M. Lyons,[1,3] Hannah Deixler,[1] Haynes Robinson,[11] David Chitayat,[12,13] Cynthia J. Curry,[14] Ralph S. Lachman,[6] William R. Wilcox,[4,6] and Deborah Krakow[1,2,5,6,]*

Fibroblast growth factor receptor 2 (FGFR2) is a crucial regulator of bone formation during embryonic development. Both gain and loss-of-function studies in mice have shown that FGFR2 maintains a critical balance between the proliferation and differentiation of osteo-progenitor cells. We have identified de novo *FGFR2* mutations in a sporadically occurring perinatal lethal skeletal dysplasia characterized by poor mineralization of the calvarium, craniosynostosis, dysmorphic facial features, prenatal teeth, hypoplastic pubis and clavicles, osteopenia, and bent long bones. Histological analysis of the long bones revealed that the growth plate contained smaller hypertrophic chondrocytes and a thickened hypercellular periosteum. Four unrelated affected individuals were found to be heterozygous for missense mutations that introduce a polar amino acid into the hydrophobic transmembrane domain of FGFR2. Using diseased chondrocytes and a cell-based assay, we determined that these mutations selectively reduced plasma-membrane levels of FGFR2 and markedly diminished the receptor's responsiveness to extracellular FGF. All together, these clinical and molecular findings are separate from previously characterized FGFR2 disorders and represent a distinct skeletal dysplasia.

Most fibroblast growth factor (FGF) ligands mediate their biological effects extracellularly by forming a complex with heparin sulfate proteoglycans and transmembrane fibroblast growth factor receptors (FGFRs). Upon activation, FGFRs autophosphorylate intracellular tyrosine residues and recruit adaptor proteins next to the membrane to launch ERK1/2, PLCγ, and PI3K/AKT cascades that subsequently regulate cell growth and differentiation.[1,2] Heterozygosity for mutations in *FGFR1*, *FGFR2*, and *FGFR3* (MIM 136350, 176943, 134934, respectively) produces a wide spectrum of genetic disorders, some with skeletal defects and others with congenital anomalies. Autosomal-dominant *FGFR2* mutations that enhance receptor signaling through ligand-independent dimerization, constitutive receptor activation, or reduced ligand specificity are responsible for craniosynostosis syndromes that include Apert syndrome (ACS1 [MIM 101200]) Crouzon syndrome (CFD1 [MIM 123500]), Jackson-Weiss syndrome (JWS [MIM 123150]), Pfeiffer syndrome (ACS5 [MIM 101600]), and Beare-Stevenson syndrome (BSTVS [MIM 123790]).[3–8] In contrast, the effect of diminished FGFR2 function in human development is seen in Lacrimoauriculodentodigital syndrome (LADD [MIM 149730]). This disorder, characterized by lacrimal-duct aplasia, dysplastic ears, hearing loss, small teeth, and digital malformations, is caused by heterozygosity for *FGFR2* mutations that reduce tyrosine kinase activity.[9,10] Although these disorders exemplify a role for FGFR2 in the development of the craniofacial complex and distal limbs, less is known about the importance of FGFR2 signaling in the remaining human appendicular skeleton.

Under an institutional review board (IRB)-approved human-subjects protocol and upon receiving informed consent, we performed a prenatal and postnatal evaluation of a fetus at 23 weeks of gestation. Our examination revealed an unusual constellation of dysmorphic features including low-set ears, hypertelorism, midface hypoplasia, micrognathia, prematurely erupted fetal teeth, and clitoromegaly (Figures 1A, 1D, and 1E and Tables 1 and 2). Radiographic findings included bent long bones, osteopenia, irregular periosteal surfaces especially in the phalanges, deficient skull ossification, coronal craniosynostosis, and hypoplastic clavicles and pubis (Figures 1H, 1J, and 1M). Subsequently, we identified three additional unrelated cases, R08-041, R96-252, and R05-427, with nearly identical clinical and radiographic findings (Figures 1B, 1C, 1F, 1G, 1I, 1K, 1L, and 1N; delineated in Tables 1 and 2). In one case (R08-041), hepatosplenomegaly with extramedullary hematopoiesis was noted at autopsy. The parents in all the families were unaffected and

[1]Department of Orthopedic Surgery, David Geffen School of Medicine, University of California, Los Angeles, Los Angeles, CA 90048, USA; [2]Human Genetics, David Geffen School of Medicine, University of California, Los Angeles, Los Angeles, CA 90048, USA; [3]Molecular Cellular and Developmental Biology, David Geffen School of Medicine, University of California, Los Angeles, Los Angeles, CA 90048, USA; [4]Pediatrics, David Geffen School of Medicine, University of California, Los Angeles, Los Angeles, CA 90048, USA; [5]Obstetrics and Gynecology, David Geffen School of Medicine, University of California, Los Angeles, Los Angeles, CA 90048, USA; [6]Medical Genetics Research Institute, Cedars-Sinai Medical Center, Los Angeles, CA 90048, USA; [7]Center for Craniofacial Molecular Biology, Ostrow School of Dentistry, University of Southern California, Los Angeles, CA 90033, USA; [8]Department of Biochemistry, Keck School of Medicine, University of Southern California, Los Angeles, CA 90033, USA; [9]Department of Animal Physiology and Immunology, Institute of Experimental Biology, Masaryk University, Brno 61265, Czech Republic; [10]Department of Cytokinetics, Institute of Biophysics Academy of Sciences of the Czech Republic, Brno 61265, Czech Republic; [11]Akron Children's Hospital, Akron, OH 44308, USA; [12]The Prenatal Diagnosis and Medical Genetics Program, Department of Obstetrics and Gynecology, Mount Sinai Hospital, Toronto, ON, M5G 1X8 Canada; [13]Department of Pediatrics, Division of Clinical and Metabolic Genetics, The Hospital for Sick Children, University of Toronto, Toronto, ON, M5G 1X8 Canada; [14]Genetic Medicine of Central California, Fresno, CA 93701, USA

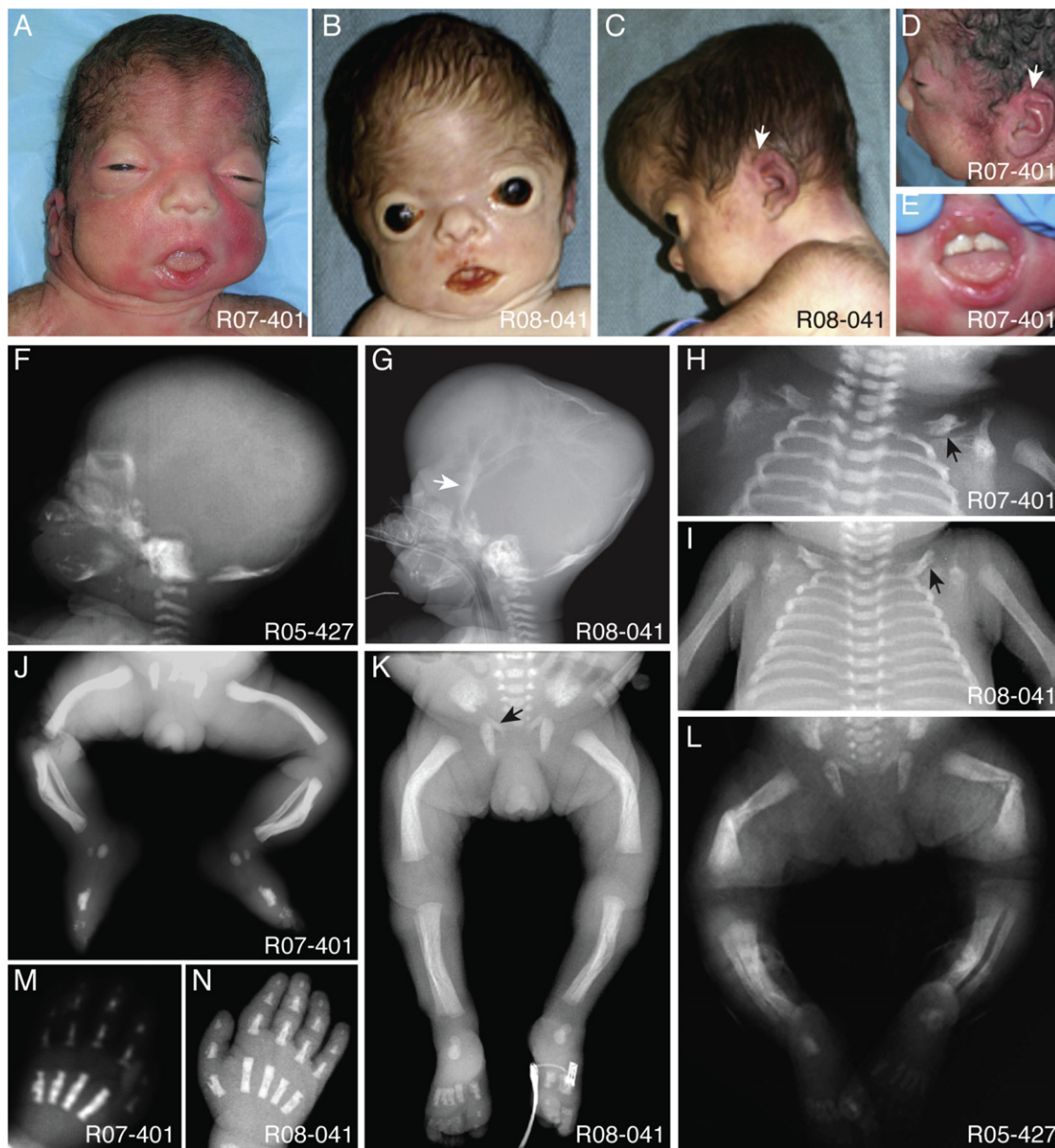*Correspondence: dkrakow@mednet.ucla.edu

Figure 1. Clinical and Radiographic Findings in BBD-FGFR2 Type
(A–E) Craniofacial abnormalities include hypertelorism, microganthia, microstomia, low-set posteriorly rotated ears, prenatal teeth, and a flattened midface.
(F–N) Radiographic analysis revealed reduced mineralization of the calvarial vault (F and G), coronal craniosynostosis (arrow in G), hypoplastic clavicles (arrows in H and I), bent long bones in the lower extremities and hypoplastic pubis (J–L, arrow in K), and boney nodules on the phalanges and metacarpals (M and N).

nonconsanguineous. In two cases (R07-401 and R08-041), a histological analysis of the long bones was performed. The distal femoral growth plate was dissected at the time of necropsy, bisected longitudinally, and embedded in plastic resin. Sections were stained with toluidine blue (the control and R07-401) or hematoxylin and eosin (R08-041). Microscopic examination showed that although there was normal organization of columnar chondrocytes, hypertrophic chondrocytes were subjectively smaller (Figures 2A–2C). The average cell size of diseased hypertrophic chondrocytes (n = 40) was measured with the public domain ImageJ[11] and found to be 0.48×

(R07-401) and 0.38× (R08-041) smaller than that found in the control. Most notably, the surrounding periosteum was thickened and hypercellular (Figures 2D–2F).

Candidate genes for mutation analysis were selected on the basis of both their expression pattern within the developing skeleton and mouse mutants with phenotypic similarities to the affected fetuses. For the following candidate genes, we amplified the coding exons from genomic DNA by using PCR (for oligonucleotide sequences, see Table S1, available online), sequenced them bidirectionally (MC Labs, San Francisco, CA), and compared them with their reference sequence by using

Table 1. Phenotypic and Radiographic Findings in Bent Bone Dysplasia-FGFR2 Type

Abnormalities	Findings
Phenotypic	
Craniofacial	open metopic suture, hypertelorism, megalophthalmos, midface hypoplasia, micrognathia, gingival hyperplasia, prenatal teeth, low-set ears, overfolded superior helix, deficient auricle
Gastrointestinal	hepatosplenomegaly with extramedullary hematopoesis
Genitourinary	clitoromegaly
Integument	hirsutism
Radiographic	
Cranium	diminished mineralization of the calvarium, craniosynostosis (coronal), midface hyoplasia, micrognathia
Thorax	bell-shaped thorax, hypoplastic clavicles, diminished mineralization of the inferior margin of the scapula
Spine	normal
Pelvis	narrow acetabular roof, narrowed ischia, diminished mineralization of the pubis
Appendicular skeleton	variable degrees of bending of the long bones, particularly of the femora, prominent periosteum
Metacarpals and phalanges	brachydactyly, areas of periosteal reaction and deficient ossification

Sequencher (Gene Codes, Ann Arbor, MI): *PRRX1* (MIM 167420), *PRRX2* (MIM 604675), *TBX15* (MIM 604127), *ALX1* (MIM 601527), *FGFR2,* and *FGFR3*. Nucleotides were numbered according to the mRNA sequence, starting from A of the ATG initiation codon. Our analysis of the 17 exons that encode *FGFR2* demonstrated that all the affected individuals were heterozygous for missense mutations within the coding region of exon 9 (RefSeq accession number NM_000141.4; Ensembl accession number ENST00000358487). Three independent cases (R07-401, R08-041, and R96-252) shared the same de novo missense mutation, c.1172T>G (Figures 3A–3C). This change pre-

Table 2. Phenotypic Spectrum among the Affected Individuals

Abnormal Findings	R08-041	R07-401	R96-252[a]	R05-427
Hypertelorism	+	+	N/A	+
Dysmorphic facies	+	+	N/A	+
Megalophthalmous	+	+	N/A	+
Prenatal teeth	−	+	N/A	−
Gastrointestinal	+	−	N/A	N/A
Clitoromegaly	+	+	N/A	+
Hirsutism	+	+	N/A	+
Hypomineralization of the calvarium	+	+	+	+
Craniosynostosis	+	+	−	+
Hypoplastic clavicles	+	+	+	+
Narrow ischia/ hypoplastic pubis	+	+	+	+
Bent long bones	+	+	+	+
Abnormal phalanges	+	+	+	+

The following abbreviation is used: N/A, not available.
[a]Only radiographs were available.

dicted the substitution p.Met391Arg (RefSeq accession number NP_000132.3), which replaces a highly conserved hydrophobic residue with a positively charged polar amino acid in the transmembrane (TM) helix (UniProt Prot P21802) (Figure 3E). The fourth affected individual, R05-427, was heterozygous for the missense mutation c.1141T>G (Figure 3D). This change predicted the substitution p.Tyr381Asp, which replaces a highly conserved hydrophobic residue with a negatively charged polar amino acid in the TM helix (Figure 3E). Mutations were not present in available parental DNA from two of the cases (R07-401 and R08-041) (Figure 3A, B) nor were they found among 210 ethnically matched control alleles. The clinical and genetic findings of these four affected individuals are distinct and constitute a distinct disorder we designate as bent bone dysplasia (BBD)-FGFR2 type.

To examine the effect of c.1172T>G on the abundance of *FGFR2* transcripts, we performed quantitative PCR (qPCR) on cDNA reverse transcribed from diseased tibia growth-plate RNA (R07-401). Specifically, we isolated RNA from the growth-plate cartilage by using Trizol (Invitrogen), synthesized cDNA by reverse transcription (Superscript, Invitrogen), and conducted qPCR by using SYBR green and primer sets spanning introns of human *Actin* (MIM 102630) and *FGFR2* (for oligonucleotide sequences, see Table S1). These experiments showed that levels of *FGFR2* transcripts from diseased growth-plate RNA were slightly higher than from that of an age-matched control (Figure 4A). We could not deduce the statistical significance of this increase because we only had access to RNA from one individual with BBD-FGFR2 type. Therefore, we concluded that *FGFR2* c.1172T>G does not lead to transcript degradation.

The TM helix of FGFR2 allows for receptor integration into the lipid bilayer during translation at the rough endoplasmic reticulum. Introduction of a polar amino acid into
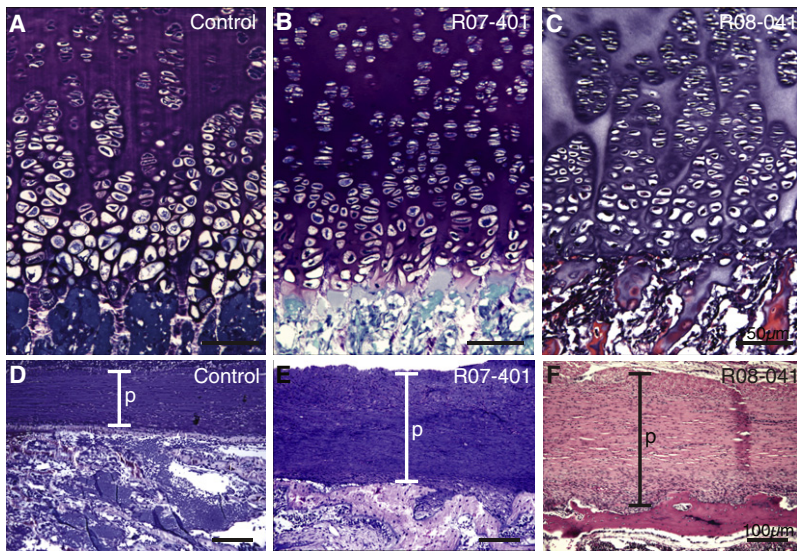
Figure 2. Histologic Analysis of the Distal Femoral Growth Plate in BBD-FGFR2 Type

Longitudinal sections through the femoral growth plate of a normal control matched for growth stage (A) and two BBD-FGFR2-type individuals, R07-401 (B) and R08-041 (C), showed that cellular organization was largely normal with subjectively smaller hypertrophic chondrocytes.

(D–F) The long-bone periosteum (p) in BBD-FGFR2-type individuals R07-401 and R08-041 was hypercellular and enlarged compared to that of the control.

a homologous region of FGFR1 decreases receptor levels at the membrane while increasing levels found in the nucleus and cytosol.[12] To determine how BBD-FGFR2-type mutations might alter secondary structure of the transmembrane domain, we analyzed the amino acid sequence for FGFR2 by using the TMHMM (transmembrane prediction based on hidden Markov models) transmembrane helices server available online through CBS Bioinformatics Tools.[13] Upon induction of p.Met391Arg or p.Tyr381Asp into FGFR2, TMHMM no longer predicted the location of the known transmembrane helix (Figures 3F–3H). This suggested that the mutations disrupt the secondary structure of the FGFR2 TM helix and prevent membrane integration. Although the hydrophobicity of the TM domain facilitates initial membrane incorporation, subsequent glycosylation of FGFR2 is critical for receptor trafficking to the cell surface.[14] To analyze the protein levels for each FGFR2 isoform in BBD-FGFR2 type, we performed immunoblots on the lysates from diseased primary chondrocytes. We liberated primary chondrocytes from the distal femurs of an affected individual (R07-401) and a staged-matched control by using 0.03% bacterial collagenase II. After a short-term culture in DMEM (Dulbecco's modified Eagle's medium) with 10% FBS, cells were lysed with RIPA (radio-immunoprecipitation assay). Protein extracts were resolved on a 10% SDS-PAGE, transferred to a nitrocellulose membrane (BioRad), and probed with the Bek antibody (FGFR2) (recognizes amino acids 771–821, Santa Cruz Biotechnology, 1/200), anti-FGFR2 extracellular (FGFR2ex) (recognizes amino acids 362–374, Sigma-Aldrich, 1/2000), or β-actin antibody (Cell Signaling Technology, 1/1000). After incubation with HRP-conjugated secondary antibody, immunoreactivity was detected with Phototope-HRP Western blot detection system (Cell Signaling Technology). Both FGFR2 antibodies were tested; one recognized the intracellular tyrosine kinase domain (FGFR2) and the other, the extracellular juxtamembrane domain (FGFR2ex), showed that

levels of the fully glycosylated receptor were reduced in diseased cells compared to control cells (Figure 4B, *bands). Biotin labeling and purification of cell-surface proteins from control and diseased chondrocytes confirmed a similar reduction in FGFR2 at the plasma membrane of diseased cells (Figure 4B) (Pierce Cell Surface Protein Isolation Kit).

The subcellular localization of FGFR2 was determined in BBD-FGFR2-type cells by immunofluorescence and confocal microscopy. Diseased and control primary chondrocytes were seeded on chamber slides (Lab-Tek), fixed in 4% paraformaldehyde for 5 min, blocked with 10% goat serum (Zymed), and incubated overnight at 4°C with either anti-Bek (FGFR2) (1/200) or anti-FGFR2 extracellular (FGFR2ex) (1/400) diluted in 1% goat serum in PBST. Primary antibodies were detected with Alexa Fluor 568 conjugated goat anti-rabbit secondary antibody diluted 1/400 in 1% goat serum in PBST. We used wheat germ agglutinin (WGA) 488 conjugate (Invitrogen) to label the plasma membrane. The FGFR2 antibody, recognizing the intracellular domain, detected receptor, marked by WGA, at the plasma membrane, and in the nuclei of control chondrocytes (Figure 4C). In BBD-FGFR2-type chondrocytes, this antibody identified very little FGFR2 at the membrane and showed that the receptor was primarily distributed in the nucleus (Figure 4D). Using the FGFR2ex antibody that recognizes the extracellular domain, we confirmed receptor localization in the plasma membrane and the nuclei of control cells (Figure 4E). In diseased cells, this antibody verified that FGFR2 was reduced at the plasma membrane, retained in the nucleus, and occasionally sequestered to juxtanuclear inclusions (Figure 4F, arrow). These inclusions, along with reduced FGFR2 glycosylation, suggest altered receptor trafficking from the endoplasmic reticulum.

We next determined the subcellular localization of mutant FGFR2^{Met391Arg} by using a cell-based assay in BaF3 cells, which lack endogenous expression of all FGF receptors and ligands.[15] Plasmids containing the cDNA for either FGFR2^{WT} or FGFR2^{Met391Arg} were introduced into BaF3 cells via the Nucleofector I device (program X-01) with Nucleofector Kit V (Amaxa, Lonza). After
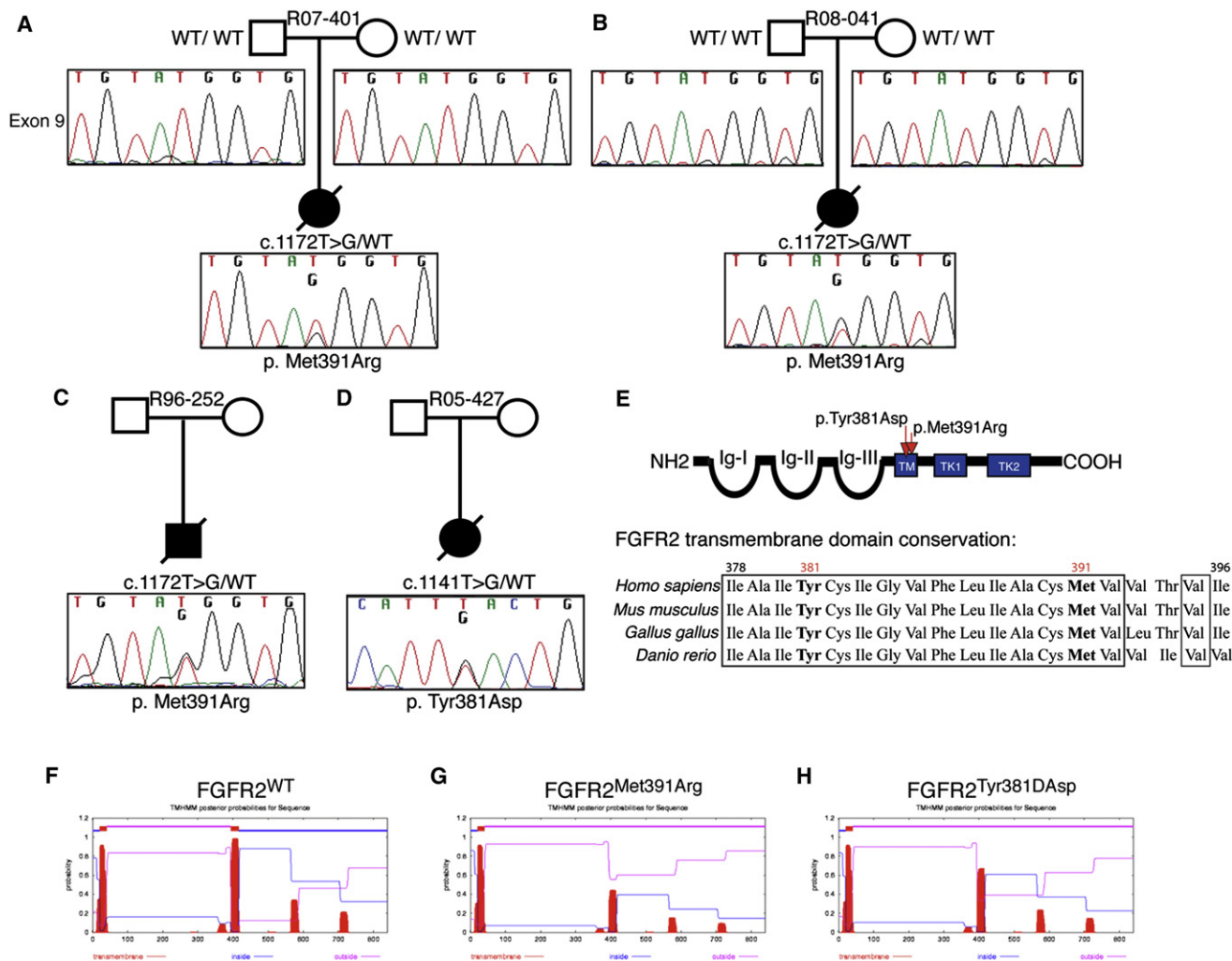
Figure 3. _FGFR2_ Mutational Analysis in BBD-FGFR2-Type Families

Sequencing chomatograms demonstrated de novo heterozygous mutations in exon 9 of _FGFR2_ in affected individuals from the four unrelated families studied. Affected individuals R07-401 (A), R08-041 (B), and R96-252 (C) shared the same de novo heterozygous mutation, c.1172T>G (p.Met391Arg).

(D) R05-427 was heterozygous for c.1141T>G (p.Tyr381Asp).

(E) All mutations (bolded) were localized to a highly conserved region within the transmembrane domain.

(F–H) TMHMM plots predicted the probability (_y_ axis) that the amino acid sequences (_x_ axis) of FGFR2, FGFR2[Met391Arg], and FGFR2[Tyr381Asp] are located outside the cell (pink bar), inside the cell (blue bar), or within the membrane (red bar).

24 hr of growth in RPMI 1640 medium (Invitrogen) supplemented with 10% newborn calf serum and murine IL-3-conditioned medium, cells were seeded on chamber slides (Lab-Tek), fixed in 4% PFA for 10 min, washed with PBS with 0.1% TritonX −100 for 30 s, and then washed three times with PBS for 15 min per wash. We then performed immunofluorescence analyses with the Bek (FGFR2) antibody and the membrane maker WGA. BaF3 cells expressing FGFR2[WT] showed receptor localization to the plasma membrane (Figure 4G), whereas the cells expressing FGFR2[Met391Arg] showed receptor restriction to the nucleus (Figure 4H).

To test if mutant FGFR2[Met391Arg] had altered responsiveness to extracellular FGF signaling, we serum-starved BaF3 cells expressing either FGFR2[WT] or FGFR2[Met391Arg] and then stimulated cells with two FGFs known to regulate

bone development.[1] After stimulation with FGF2 (MIM 134920) or FGF18 (MIM 603726) (100 ng/ml of ligand with 10 μg/ml heparin; R&D Systems, Peprotech) for 30 min, we lysed cells and analyzed levels of phosphorylated ERK1/2 (p-ERK1/2), a canonical target of FGF signaling in bone, by immunoblot analyses. Membranes probed with anti-p-ERK1/2 (Cell Signaling Technology, 1/1000) and anti-α-tubulin (Cell Signaling Technology, 1/1000) showed that, unlike FGFR2[WT]-expressing cells, FGFR2[Met391Arg]-expressing cells are unable to activate phosphorylation of ERK1/2 (Figure 4I). Lack of FGF responsiveness by FGFR2[Met391Arg] suggests that BBD-FGFR2 type, in part, results from reduced FGFR2 signaling at the plasma membrane.

The clinical and radiographic findings in this FGFR2 syndrome are separate from the other well-established

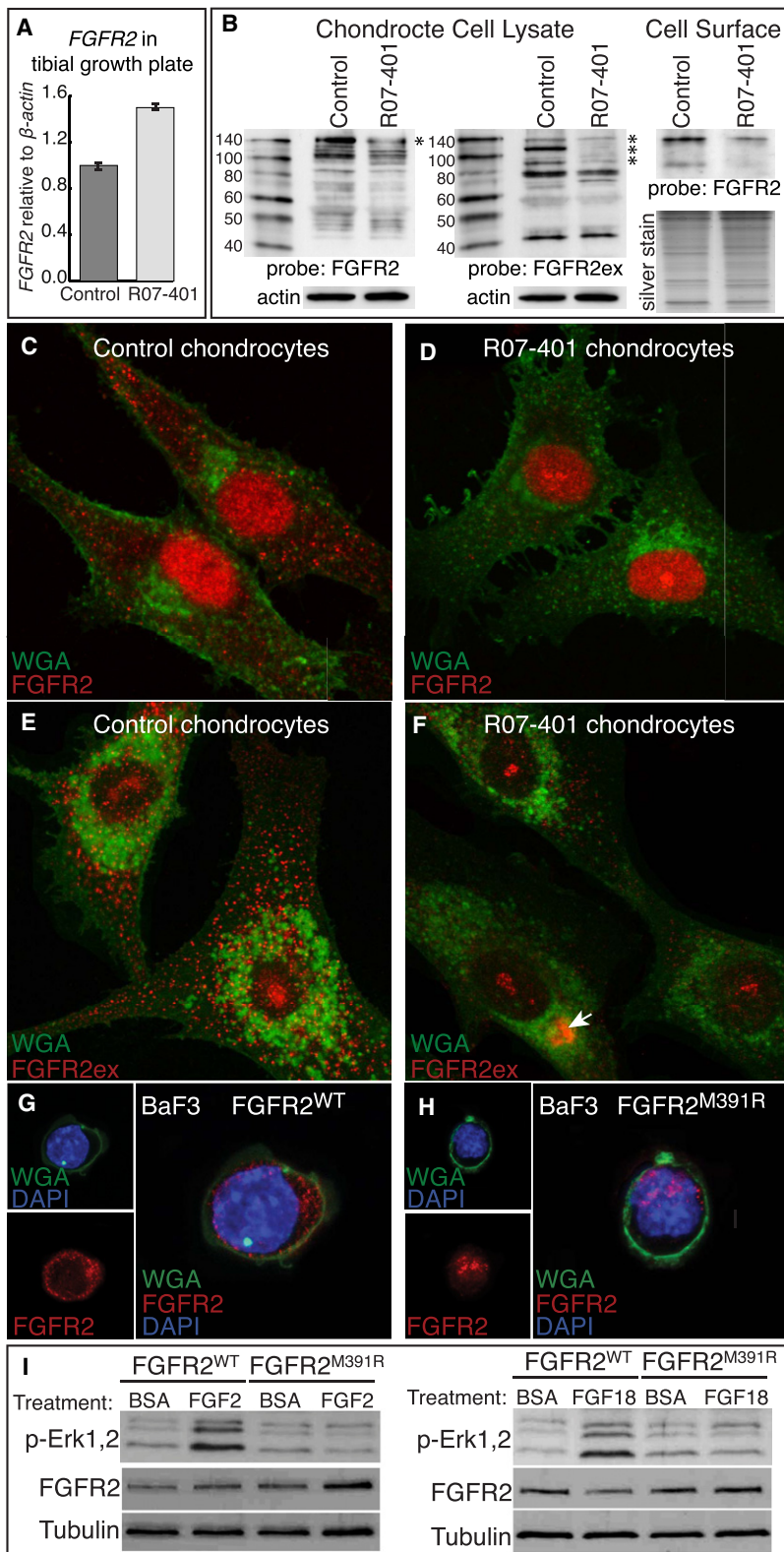**Figure 4. Mutant FGFR2^Met391Arg Showed Deficient Plasma-Membrane Localization and Reduced Responsiveness to Extracellular FGF**

(A) Quantitative PCR of tibial growth-plate cDNA in the control and R07-401 showed that R07-401 had slightly elevated levels of *FGFR2* expression.

(B) Immunoblot analysis—with FGFR2 antibodies that recognize either the intracellular domain (anti-FGFR2) or extracellular domain (anti-FGFR2ex) of total lysates from primary chondrocytes showed that there were fewer highly glycosylated forms of FGFR2 in R07-401 chondrocytes than in the control (*bands). Biotin labeling and purification of cell-surface proteins identified less surface FGFR2 in R07-401 cells than in the control.

(C) Immunofluorescent detection with an antibody recognizing the intracellular domain of FGFR2 (red) and the membrane marker WGA (green) in primary chondrocytes localized FGFR2 to the membrane and nuclei of control chondrocytes.

(D) Although membrane localization was undetectable in R07-401 cells, nuclear receptor levels were retained.

(E) The FGFR2ex antibody detected receptor in the plasma membrane and nuclei of control cells.

(F) In R07-401 cells, the FGFR2ex antibody detected receptor in the nuclei and juxtanuclear intracellular inclusions (arrow).

(G and H) BaF3 cells overexpressing either wild-type or mutant FGFR2 were immuolabeled for FGFR2 (red) and WGA (green) and showed that FGFR2^WT localized to the membrane whereas FGFR2^Met391Arg was restricted to the nucleus (blue).

(I) Immunoblot analysis of lysates from BaF3 cells overexpressing FGFR2^WT or FGFR2^Met391Arg showed that FGFR2^Met391Arg-expressing cells were unable to induce phosphorylation of ERK1/2 upon 30 min of stimulation with either FGF2 or FGF18.

skeletal defects in BBD-FGFR2 type are particularly profound and distinct. Among the nonskeletal abnormalities in BBD-FGFR2 type, clitoromegally was seen in three unrelated individuals with female karyotypes. Although hypogonadism and genitourinary abnormalities result from loss of FGFR1 function in Kallmann syndrome (KAL2 [MIM 136350]),[16] these particular findings have not been previously described in the FGFR2 disorders. FGF signaling plays a key role in the development of the genital tubercle. For example, FGF10 (MIM 602115), a ligand for FGFR2, is critical for the outgrowth of the genital tubercle. *Fgf10*-deficient mice have morphologic defects in the urethral epithelium and prepuce.[17] Therefore, the genital abnormalities found in three independent BBD-FGFR2-type cases might be mechanistically linked to disturbances in FGF signaling during genitalia development.

FGFR2 syndromes and represent a distinct skeletal dysplasia. Previously recognized FGFR2 disorders manifest postnatal growth disturbances associated with mild short stature, craniosynostosis, radioulnar synostosis, and hand and foot abnormalities; however, the appendicular

The skeletal abnormalities seen in BBD-FGFR2 type support a necessary role for FGFR2 signaling during endochondral and intramembranous bone formation. The fact that these abnormalities, at least partially, result from deficient FGFR2 signaling in the plasma membrane is further supported by loss-of-function studies in mice. Although complete *Fgfr2* deficiency in mice causes embryonic lethality,[18,19] conditional inactivation of the receptor in skeletogenic mesenchyme (*Dermo1-Cre*) causes a dome-shaped skull and longitudinal shortening of axial and appendicular skeletal elements.[20] The two major *FGFR2* transcriptional variants, generated by alternative splicing of the ligand-binding domain, have distinct roles during bone formation. The TM domain is conserved between these variants, and the mutations identified in BBD-FGFR2 type are therefore predicted to disrupt the function of both FGFR2 isoforms. This is supported by the phenotypic similarities between BBD-FGFR2 type and mice with selective inactivation of each FGFR2 splice variant. Selective ablation of the epithelial-specific splice variant *Fgfr2-IIIb* results in severe reduction of the scapula, malformation of the clavicles, and absence of the pubis.[21–23] Mice selectively deficient in the mesenchyme-specific splice variant *Fgfr2-IIIc* have delayed mineralization of the calvarium, craniosynostosis, and shortened long bones.[24] Therefore, this skeletal phenotype of BBD-FGFR2 type most likely results from altered FGFR2 signaling in both epithelial- and mesenchymal-derived tissues during bone formation.

Both gain and loss-of-function studies have shown that FGFR2 maintains a balance between the proliferation and differentiation of osteoprogenitor cells—loss leads to decreased proliferation and differentiation,[20,21,24] and gain leads to enhanced proliferation and differentiation.[25,26] Interestingly, the BBD-FGFR2-type skeletal phenotype shows some evidence of receptor gain of function: The periosteum, a principal source of osteoprogenitor cells, is hypercellular and enlarged. Furthermore, few phenotypic similarities between BBD-FGFR2 type and LADD syndrome support the idea that the abnormalities in BBD-FGFR2 type do not uniformly result from a strict loss of FGFR2 function. An explanation for this conundrum might lie within the less-understood intracellular signaling role for FGFRs. Although the FGFR2 mutations identified in BBD-FGFR2 type lead to deficiency in plasma-membrane targeting, our data show that nuclear FGFR2 in cells remains unaltered. It thus remains a possibility that the mutant FGFR2 retains intracellular activity. For example, it has been previously revealed that unglycosylated FGFR2, despite deficient targeting to the plasma membrane, activates the PLCγ pathway through intracellular mechanisms.[14] Dissimilarities between BBD-FGFR2 type and the established FGFR2 disorders suggest that these distinct mutations will provide new insight into FGF signaling not previously understood by a strict gain or loss of FGFR2 function. Further studies with the use of mouse models and cell-based assays will help us resolve how distinct cellular-signaling routes for FGFR2 influence the phenotypic complexities of this human skeletal disorder.

Web Resources

The URLs for data presented herein are as follows:

ImageJ Software, http://rsb.info.nih.gov/ij/
Online Mendelian Inheritance in Man (OMIM), http://www.omim.org
TMHMM Server v. 2.0, http://www.cbs.dtu.dk/services/TMHMM/

References

1. Ornitz, D.M., and Marie, P.J. (2002). FGF signaling pathways in endochondral and intramembranous bone development and human genetic disease. Genes Dev. *16*, 1446–1465.
2. Eswarakumar, V.P., Lax, I., and Schlessinger, J. (2005). Cellular signaling by fibroblast growth factor receptors. Cytokine Growth Factor Rev. *16*, 139–149.
3. Mangasarian, K., Li, Y., Mansukhani, A., and Basilico, C. (1997). Mutation associated with Crouzon syndrome causes ligand-independent dimerization and activation of FGF receptor-2. J. Cell. Physiol. *172*, 117–125.
4. Meyers, G.A., Day, D., Goldberg, R., Daentl, D.L., Przylepa, K.A., Abrams, L.J., Graham, J.M., Jr., Feingold, M., Moeschler, J.B., Rawnsley, E., et al. (1996). FGFR2 exon IIIa and IIIc mutations in Crouzon, Jackson-Weiss, and Pfeiffer syndromes: Evidence for missense changes, insertions, and a deletion due to alternative RNA splicing. Am. J. Hum. Genet. *58*, 491–498.
5. Lajeunie, E., Heuertz, S., El Ghouzzi, V., Martinovic, J., Renier, D., Le Merrer, M., and Bonaventure, J. (2006). Mutation screening in patients with syndromic craniosynostoses indicates that a limited number of recurrent FGFR2 mutations accounts for severe forms of Pfeiffer syndrome. Eur. J. Hum. Genet. *14*, 289–298.

6. Galvin, B.D., Hart, K.C., Meyer, A.N., Webster, M.K., and Donoghue, D.J. (1996). Constitutive receptor activation by Crouzon syndrome mutations in fibroblast growth factor receptor (FGFR)2 and FGFR2/Neu chimeras. Proc. Natl. Acad. Sci. USA *93*, 7894–7899.

7. Robertson, S.C., Meyer, A.N., Hart, K.C., Galvin, B.D., Webster, M.K., and Donoghue, D.J. (1998). Activating mutations in the extracellular domain of the fibroblast growth factor receptor 2 function by disruption of the disulfide bond in the third immunoglobulin-like domain. Proc. Natl. Acad. Sci. USA *95*, 4567–4572.

8. Yu, K., Herr, A.B., Waksman, G., and Ornitz, D.M. (2000). Loss of fibroblast growth factor receptor 2 ligand-binding specificity in Apert syndrome. Proc. Natl. Acad. Sci. USA *97*, 14536–14541.

9. Rohmann, E., Brunner, H.G., Kayserili, H., Uyguner, O., Nürnberg, G., Lew, E.D., Dobbie, A., Eswarakumar, V.P., Uzumcu, A., Ulubil-Emeroglu, M., et al. (2006). Mutations in different components of FGF signaling in LADD syndrome. Nat. Genet. *38*, 414–417.

10. Lew, E.D., Bae, J.H., Rohmann, E., Wollnik, B., and Schlessinger, J. (2007). Structural basis for reduced FGFR2 activity in LADD syndrome: Implications for FGFR autoinhibition and activation. Proc. Natl. Acad. Sci. USA *104*, 19802–19807.

11. McAtee, P.A., Hallett, I.C., Johnston, J.W., and Schaffer, R.J. (2009). A rapid method of fruit cell isolation for cell size and shape measurements. Plant Methods *5*, 5.

12. Myers, J.M., Martins, G.G., Ostrowski, J., and Stachowiak, M.K. (2003). Nuclear trafficking of FGFR1: A role for the transmembrane domain. J. Cell. Biochem. *88*, 1273–1291.

13. Krogh, A., Larsson, B., von Heijne, G., and Sonnhammer, E.L. (2001). Predicting transmembrane protein topology with a hidden Markov model: Application to complete genomes. J. Mol. Biol. *305*, 567–580.

14. Hatch, N.E., Hudson, M., Seto, M.L., Cunningham, M.L., and Bothwell, M. (2006). Intracellular retention, degradation, and signaling of glycosylation-deficient FGFR2 and craniosynostosis syndrome-associated FGFR2C278F. J. Biol. Chem. *281*, 27292–27305.

15. Mathieu, M., Chatelain, E., Ornitz, D., Bresnick, J., Mason, I., Kiefer, P., and Dickson, C. (1995). Receptor binding and mitogenic properties of mouse fibroblast growth factor 3. Modulation of response by heparin. J. Biol. Chem. *270*, 24197–24203.

16. Dodé, C., Levilliers, J., Dupont, J.M., De Paepe, A., Le Dû, N., Soussi-Yanicostas, N., Coimbra, R.S., Delmaghani, S., Compain-Nouaille, S., Baverel, F., et al. (2003). Loss-of-function mutations in FGFR1 cause autosomal dominant Kallmann syndrome. Nat. Genet. *33*, 463–465.

17. Haraguchi, R., Suzuki, K., Murakami, R., Sakai, M., Kamikawa, M., Kengaku, M., Sekine, K., Kawano, H., Kato, S., Ueno, N., and Yamada, G. (2000). Molecular analysis of external genitalia formation: The role of fibroblast growth factor (Fgf) genes during genital tubercle formation. Development *127*, 2471–2479.

18. Arman, E., Haffner-Krausz, R., Chen, Y., Heath, J.K., and Lonai, P. (1998). Targeted disruption of fibroblast growth factor (FGF) receptor 2 suggests a role for FGF signaling in pregastrulation mammalian development. Proc. Natl. Acad. Sci. USA *95*, 5082–5087.

19. Xu, X., Weinstein, M., Li, C., Naski, M., Cohen, R.I., Ornitz, D.M., Leder, P., and Deng, C. (1998). Fibroblast growth factor receptor 2 (FGFR2)-mediated reciprocal regulation loop between FGF8 and FGF10 is essential for limb induction. Development *125*, 753–765.

20. Yu, K., Xu, J., Liu, Z., Sosic, D., Shao, J., Olson, E.N., Towler, D.A., and Ornitz, D.M. (2003). Conditional inactivation of FGF receptor 2 reveals an essential role for FGF signaling in the regulation of osteoblast function and bone growth. Development *130*, 3063–3074.

21. De Moerlooze, L., Spencer-Dene, B., Revest, J.M., Hajihosseini, M., Rosewell, I., and Dickson, C. (2000). An important role for the IIIb isoform of fibroblast growth factor receptor 2 (FGFR2) in mesenchymal-epithelial signalling during mouse organogenesis. Development *127*, 483–492.

22. Revest, J.M., Spencer-Dene, B., Kerr, K., De Moerlooze, L., Rosewell, I., and Dickson, C. (2001). Fibroblast growth factor receptor 2-IIIb acts upstream of Shh and Fgf4 and is required for limb bud maintenance but not for the induction of Fgf8, Fgf10, Msx1, or Bmp4. Dev. Biol. *231*, 47–62.

23. Celli, G., LaRochelle, W.J., Mackem, S., Sharp, R., and Merlino, G. (1998). Soluble dominant-negative receptor uncovers essential roles for fibroblast growth factors in multi-organ induction and patterning. EMBO J. *17*, 1642–1655.

24. Eswarakumar, V.P., Monsonego-Ornan, E., Pines, M., Antonopoulou, I., Morriss-Kay, G.M., and Lonai, P. (2002). The IIIc alternative of Fgfr2 is a positive regulator of bone formation. Development *129*, 3783–3793.

25. Eswarakumar, V.P., Horowitz, M.C., Locklin, R., Morriss-Kay, G.M., and Lonai, P. (2004). A gain-of-function mutation of Fgfr2c demonstrates the roles of this receptor variant in osteogenesis. Proc. Natl. Acad. Sci. USA *101*, 12555–12560.

26. Wang, Y., Xiao, R., Yang, F., Karim, B.O., Iacovelli, A.J., Cai, J., Lerner, C.P., Richtsmeier, J.T., Leszl, J.M., Hill, C.A., et al. (2005). Abnormalities in cartilage and bone development in the Apert syndrome FGFR2(+/S252W) mouse. Development *132*, 3537–3548.